Terahertz optical properties of potassium titanyl phosphate crystals

V. D. Antsygin,[1] A. B. Kaplun,[2] A. A. Mamrashev,[1,*] N. A. Nikolaev,[1] and O. I. Potaturkin[1, 3]

[1]*Institute of Automation & Electrometry, the Siberian Branch of the Russian Academy of Sciences, 1 Ac. Koptyuga Av., Novosibirsk, 630090, Russia*
[2]*Institute of Thermophysics, the Siberian Branch of the Russian Academy of Sciences, 1 Ac. Lavrentyeva Av., Novosibirsk, 630090, Russia*
[3]*Novosibirsk State University, 2 Pirogova Str., Novosibirsk, 630090, Russia*
**mamrashev@iae.nsk.su*

Abstract: This paper studies the terahertz optical properties of nonlinear potassium titanyl phosphate crystals with different conductivities in the spectral range of 0.2 to 2.6 THz. The observed properties are characterized by several absorption lines lying along different optical axes which represent the relevant potassium sublattice phonon modes. The peculiarities of these absorption lines are attributed to the structural order of potassium ions.

OCIS codes: (300.6495) Spectroscopy, terahertz; (260.1180) Crystal optics.

References and links

1. M. N. Satyanarayan, A. Deepthy, and H. L. Bhat, "Potassium titanyl phosphate and its isomorphs: growth, properties, and applications," Crit. Rev. Solid State Mater. Sci. **24**(2), 103–191 (1999).
2. M. Roth, N. Angert, M. Tseitlin, and A. Alexandrovski, "On the optical quality of KTP crystals for nonlinear optical and electro-optic applications," Opt. Mater. **16**(1-2), 131–136 (2001).
3. N. I. Sorokina and V. I. Voronkova, "Structure and properties of crystals in the potassium titanyl phosphate family: A review," Crystallogr. Rep. **52**(1), 80–93 (2007).
4. A. H. Reshak, I. V. Kityk, and S. Auluck, "Investigation of the linear and nonlinear optical susceptibilities of $KTiOPO_4$ single crystals: theory and experiment," J. Phys. Chem. B **114**(50), 16705–16712 (2010).
5. M. V. Pack, D. J. Armstrong, and A. V. Smith, "Measurement of the $\chi^{(2)}$ tensors of $KTiOPO_4$, $KTiOAsO_4$, $RbTiOPO_4$, and $RbTiOAsO_4$ crystals," Appl. Opt. **43**(16), 3319–3323 (2004).
6. D. Xue and S. Zhang, "The origin of nonlinearity in $KTiOPO_4$," Appl. Phys. Lett. **70**(8), 943–945 (1997).
7. A. Englander, R. Lavi, M. Katz, M. Oron, D. Eger, E. Lebiush, G. Rosenman, and A. Skliar, "Highly efficient doubling of a high-repetition-rate diode-pumped laser with bulk periodically poled KTP," Opt. Lett. **22**(21), 1598–1599 (1997).
8. R. Le Targat, J.-J. Zondy, and P. Lemonde, "75%-efficiency blue generation from an intracavity PPKTP frequency doubler," Opt. Commun. **247**(4-6), 471–481 (2005).
9. G. K. Samanta, S. C. Kumar, M. Mathew, C. Canalias, V. Pasiskevicius, F. Laurell, and M. Ebrahim-Zadeh, "High-power, continuous-wave, second-harmonic generation at 532 nm in periodically poled $KTiOPO_4$," Opt. Lett. **33**(24), 2955–2957 (2008).
10. B. Agate, E. U. Rafailov, W. Sibbett, S. M. Saltiel, P. Battle, T. Fry, and E. Noonan, "Highly efficient blue-light generation from a compact, diode-pumped femtosecond laser by use of a periodically poled KTP waveguide crystal," Opt. Lett. **28**(20), 1963–1965 (2003).
11. N. Dong, F. Chen, and J. R. Vázquez de Aldana, "Efficient second harmonic generation by birefringent phase matching in femtosecond-laser-inscribed KTP cladding waveguides," Phys. Status Solidi RRL-Rapid Res. Lett. **6**, 306–308 (2012).
12. F. Laurell, T. Calmano, S. Müller, P. Zeil, C. Canalias, and G. Huber, "Laser-written waveguides in KTP for broadband Type II second harmonic generation," Opt. Express **20**(20), 22308–22313 (2012).
13. T. Taniuchi, S. Okada, and H. Nakanishi, "Widely tunable terahertz-wave generation in an organic crystal and its spectroscopic application," J. Appl. Phys. **95**(11), 5984–5988 (2004).
14. B. Wyncke, F. Brehat, J. Mangin, G. Marnier, M. F. Ravet, and M. Metzger, "Infrared reflectivity spectrum of $KTiOPO_4$ single crystal," Phase Transit. **9**(2), 179–183 (1987).
15. G. E. Kugel, F. Brehat, B. Wyncke, M. D. Fontana, G. Marnier, C. Carabatos-Nedelec, and J. Mangin, "The vibrational spectrum of a $KTiOPO_4$ single crystal studied by Raman and infrared reflectivity spectroscopy," J. Phys. C Solid State Phys. **21**(32), 5565–5583 (1988).
16. K. Vivekanandan, S. Selvasekarapandian, P. Kolandaivel, M. T. Sebastian, and S. Suma, "Raman and FT-IR spectroscopic characterisation of flux grown $KTiOPO_4$ and $KRbTiOPO_4$ non-linear optical crystals," Mater. Chem. Phys. **49**(3), 204–210 (1997).

#222577 - $15.00 USD Received 8 Sep 2014; accepted 18 Sep 2014; published 10 Oct 2014

17. H.-R. Xia, L.-X. Li, and J.-Y. Wang, "The features of lattice vibration of KTP single crystal," Acta Phys. Sin. **45**, 1159–1166 (1996).
18. P. Mounaix, L. Sarger, J. P. Caumes, and E. Freysz, "Characterization of non-linear potassium crystals in the terahertz frequency domain," Opt. Commun. **242**(4-6), 631–639 (2004).
19. M. Sang, L. Fan, X. Lu, and W. Zhang, "Optical phonon resonance of KTiOP04 crystal characterized by THz time-domain spectroscopy," Acta Photonica Sin. **32**, 1286–1290 (2009).
20. V. D. Antsygin, A. A. Mamrashev, N. A. Nikolaev, and O. I. Potaturkin, "Small-size terahertz spectrometer using the second harmonic of a femtosecond fiber laser," Optoelectron. Instrum. Data Process. **46**(3), 294–300 (2010).
21. V. A. Rusov, V. A. Serebryakov, A. B. Kaplun, and A. V. Gorchakov, "Using modulators based on KTP crystals in Nd:YAG lasers with high mean power," J. Opt. Technol. **76**(6), 325 (2009).
22. W. Withayachumnankul, B. M. Fischer, and D. Abbott, "Material thickness optimization for transmission-mode terahertz time-domain spectroscopy," Opt. Express **16**(10), 7382–7396 (2008).
23. L. Duvillaret, F. Garet, and J. L. Coutaz, "A reliable method for extraction of material parameters in terahertz time-domain spectroscopy," IEEE J. Sel. Top. Quantum Electron. **2**(3), 739–746 (1996).
24. V. D. Antsigin, V. A. Gusev, V. N. Semenenko, and A. M. Yurkin, "Ferroelectric and nonlinear optical properties of ferroelectric-superionic KTP," Ferroelectrics **143**(1), 223–227 (1993).
25. F. K. Larsen, "Diffraction studies of crystals at low temperatures – crystallography below 77 K," Acta Crystallogr. B **51**(4), 468–482 (1995).
26. N. E. Novikova, I. A. Verin, N. I. Sorokina, O. A. Alekseeva, M. Tseitlin, and M. Roth, "Structure of $KTiOAsO_4$ single crystals at 293 and 30 K," Crystallogr. Rep. **55**(3), 412–423 (2010).

1. Introduction

Potassium titanyl phosphate crystal ($KTiOPO_4$, KTP) [1–3] is a popular nonlinear optical material used for frequency conversion, as it has high nonlinear-optical coefficients, a wide transparency range of 0.35 to 4.5 μm and a high damage threshold of up to 15 GW/cm^2 [4–6]. Its large electro-optic coefficients and low dielectric constants also make it suitable for the manufacturing of efficient optical modulators and Q-switches. Periodic polarization [7–9] and waveguide manufacturing [10–12] are utilized to enhance the nonlinear light conversion efficiency of KTP crystals. KTP is also used as a material for optical parametric oscillators (OPOs) and amplifiers.

KTP-based OPOs could be used to generate tunable narrowband terahertz radiation in organic materials [13]. However, any direct terahertz applications of KTP crystals require detailed knowledge of their optical properties in the terahertz region. These characteristics were investigated by the methods of Raman scattering and infrared reflection spectroscopy – although very scarcely [14–17], unlike the well-studied properties in the IR, visible and UV spectral ranges. The recent introduction of time-domain terahertz spectroscopy has made it possible to perform the initial measurements of KTP absorption coefficients and refractive indices at frequencies of up to 2 THz [18,19].

We report the optical properties of KTP single crystals with different conductivities in the spectral range of 0.2 to 2.6 THz along different optical axes measured by a conventional terahertz time-domain spectroscopy (THz-TDS) system [20].

2. Experimental setup and sample details

In our THz-TDS setup the radiation of the second harmonic of the Er-doped fiber laser is used to generate terahertz radiation in an interdigitated photoconductive antenna (Batop Optics, Germany). Electrooptic sampling in 1 mm-thick ZnTe crystals with antireflection coating is used for terahertz radiation detection. The generated terahertz radiation is contained in a gas cell pumped with dry nitrogen, so as to exclude the influence of atmospheric water vapor. The investigated samples can also be put in a cryostat and cooled down to 80 K.

We studied samples from three ingots (Single Crystals LLC, Russia) grown from polyphosphate solution-melts. A modified Czochralski method was used for the growth, with the seed crystal oriented along *x*-axis in a gradient temperature field. Vibrational methods of viscosity measurements and phase analysis were used to control melt characteristics and crystallization parameters. It allowed choosing optimal flux composition and optimum process regimes for growing crystals with specified properties. In particular, it allowed adjusting electrical conductivity along the *z*-axis. It is considered to be a major generic parameter of KTP crystals as it gives information about their perfection and defines the main

#222577 - $15.00 USD Received 8 Sep 2014; accepted 18 Sep 2014; published 10 Oct 2014

technical properties of KTP-based devices. For instance, crystals with lower conductivity have higher electrical and radiation resistance [21].

The studied samples had different direct current conductivity along the *z*-axis: $\sigma_1 = 2\cdot10^{-6}$ $Ohm^{-1}\cdot cm^{-1}$ (low-resistivity, LR crystals), $\sigma_2 \approx 10^{-11}$ $Ohm^{-1}\cdot cm^{-1}$ (high-resistivity, HR crystals) and $\sigma_3 \approx 10^{-12}$ $Ohm^{-1}\cdot cm^{-1}$ (super-high resistivity, SHR crystals). The LR samples were *y*-cut and 355-μm-thick. The HR samples were *x*-cut and *y*-cut, which enabled us to measure their terahertz properties along all three optical axes, and had a thickness of ca 275 μm. The SHR crystal at our disposal was *x*-cut only. After initial investigation, the sample crystals were optically polished down to a thickness of about 70–80 μm, so that their properties could be studied at spectral ranges with higher absorption [22]. The measurements for the thick and thin samples were then juxtaposed to represent the optical properties of the crystals at THz region in the most comprehensive way.

KTP is an orthorhombic crystal belonging to the space group $Pna2_1$. Since the investigated crystals are biaxial, the measurements of their terahertz transmission were performed in two stages. First, the optical axis *z* of the crystals was aligned perpendicularly to the terahertz wave polarization, which made it possible to measure THz transmission along the *x*- and *y*-axes. Next, it was aligned in parallel to the terahertz wave polarization (transmission along the *z*-axis). Time-domain terahertz signals and corresponding power spectra of typical reference and sample pulses can be seen in Fig. 1.

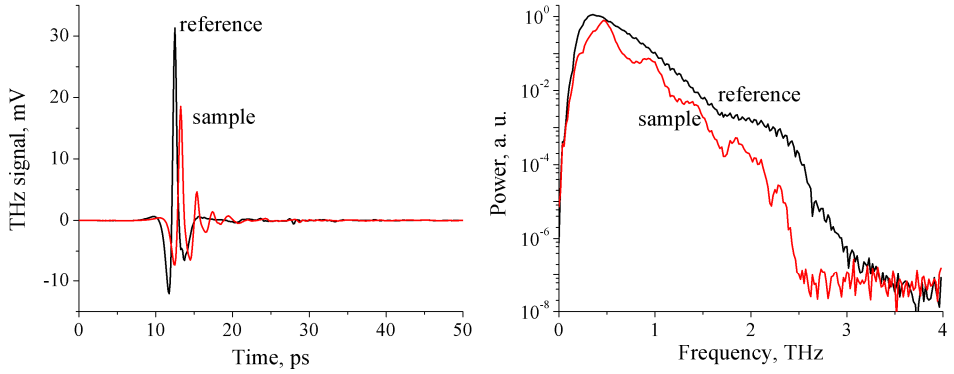

Fig. 1. Time-domain terahertz pulses (left) and corresponding frequency-domain power spectra (right).

The optical properties and thickness of the samples were calculated with the help of the parameters extraction method on the basis of transmission measurement data [23]. Calculations of uncertainties of absorption and refractive index were based on a series of measurements using procedure from [22] by Withayachumnankul et al. The accuracy of the sample thickness estimated on the order of 1 μm allowed us to carry out the refractive index measurements with an uncertainty of less than 0.003. As a result, the complex refractive index $\hat{n} = n + i\kappa$ was obtained consisting of the real part *n* (a refractive index) and the imaginary part κ (an extinction coefficient). Absorption coefficient α and complex dielectric permittivity ε were then derived from the complex refractive index using the following expressions:

$$\alpha = \frac{2\kappa\omega}{c}; \tag{1}$$

$$\varepsilon = (n + i\kappa)^2 = (n^2 - \kappa^2) + 2in\kappa. \tag{2}$$

The optical properties observed along different optical axes were denoted by the corresponding subscripts (*x*, *y* and *z*).

#222577 - $15.00 USD Received 8 Sep 2014; accepted 18 Sep 2014; published 10 Oct 2014

3. Results and discussions

The most comprehensive optical properties data – the refractive indices and absorption – were obtained for the HR crystals at room temperature of 296 K (see Fig. 2). Several absorption lines can be clearly seen in this figure. Refractive index shows dispersive-like features corresponding to the pronounced absorption peaks. The crystals exhibit high birefringence of $\Delta n = n_z - n_y \approx 0.65$ which doesn't change in the frequency range up to 1.4 THz where the influence of 1.73 THz absorption line becomes significant. Similarly, the difference between refractive indices along *x*- and *y*-axes remains constant and equal to 0.05 up to the vicinity of 2.15 THz absorption line.

The measured absorption could be fitted using the Voigt and Lorentzian peak functions with almost the same accuracy. That is why we used a simpler Lorentzian approximation based on the following formula:

$$\alpha(f) = \sum_i \frac{2A_i w_i}{\pi\left(4(f - f_i)^2 + w_i^2\right)}, \tag{3}$$

where A_i, w_i, f_i are the amplitude, width and central frequency of the *i*-th phonon mode. Resulting fitting curves are presented in Fig. 2 along with the measured curves.

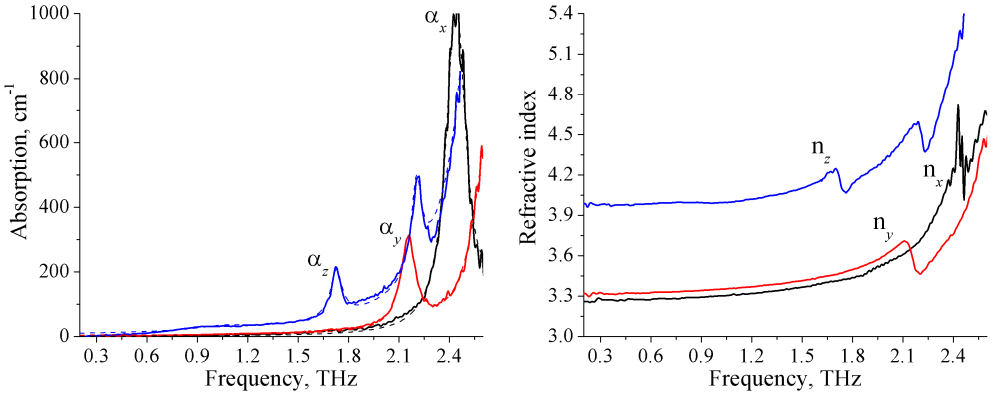

Fig. 2. Terahertz absorption (left) and refractive indices (right) of high-resistivity KTP crystals at room temperature of 296 K. Dashed lines represent Lorentz approximation.

The next Fig. 3 compares absorption and refractive indices of HR and LR crystals along the *x*-axis. Absorption is characterized by a pronounced phonon line at 2.44 THz. One more line at roughly 2.69 THz was measured at the limits of spectrometer capabilities, i. e. with less accuracy, and it was not plotted in Fig. 3. The measured lines were fitted using the same Lorentzian peak function of Eq. (3) (see Table 1 for results). It can be seen that the central frequency of the lowest phonon mode shifts to a lower range by no more than 5 GHz for the LR crystals, as compared to the HR crystals, and their width is almost equal. The difference between refractive indices of the crystals is about 0.04. The observed difference is accounted for the inequality of amplitude and width of 2.44 THz absorption line of HR and LR crystals.

Terahertz properties of HR and SHR crystals and results of absorption fitting are presented in Fig. 4 and Table 2 correspondingly. SHR phonon absorption line at 2.62 THz is weaker and narrower than that of HR crystal. This peculiarity explains the fact that refractive index is lower by about 0.17 in SHR crystal compared to HR at frequencies below 2 THz.

#222577 - $15.00 USD Received 8 Sep 2014; accepted 18 Sep 2014; published 10 Oct 2014

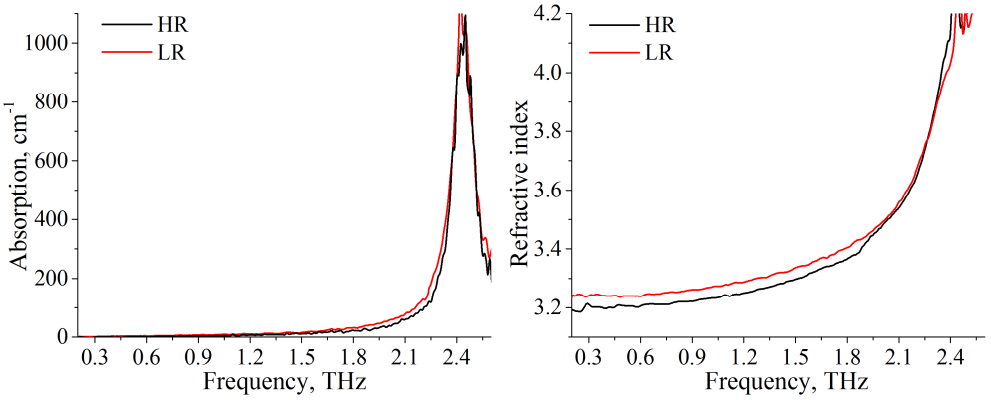

Fig. 3. Terahertz absorption (left) and refractive indices (right) of LR and HR crystals along the *x*-axis.

Table 1. Comparison of characteristics of two phonon lines along *x*-axis for HR and LR crystals at room temperature

Crystal	f_1, THz	w_1, THz	A_1, 10^3 THz/m	f_2, THz	w_2, THz	A_2, 10^3 THz/m
LR	2.434	0.15	25.4	2.69*	0.098*	5.4*
HR	2.439	0.143	23	2.67*	0.091*	4.5*

*The specified line was measured at the limits of spectrometer capabilities and its properties are considered less accurate due to higher noise beyond the investigated range of 0.2 to 2.6 THz. The data in the table are presented to the last significant digit.

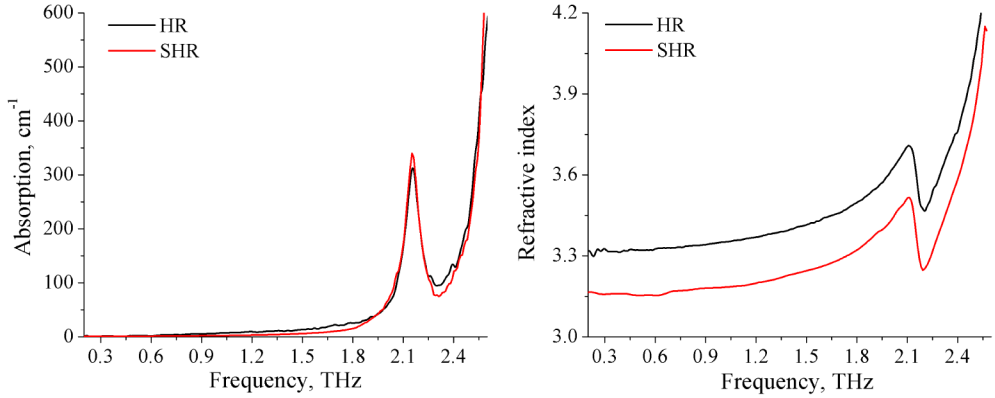

Fig. 4. Terahertz absorption (left) and refractive indices (right) of HR and SHR crystals along the *y*-axis.

Table 2. Comparison of characteristics of two phonon lines along y-axis for HR and SHR crystals at room temperature

Crystal	f_1, THz	w_1, THz	A_1, 10^3 THz/m	f_2, THz	w_2, THz	A_2, 10^3 THz/m
HR	2.154	0.112	4.8	2.64*	0.22*	22.0*
SHR	2.152	0.111	5.2	2.62*	0.16*	17.1*

*Position, width and amplitude of this peak were estimated using fitting of the left slope of the absorption line.
The data in the table are presented to the last significant digit.

The most peculiar properties are exhibited by KTP crystals along the *z*-axis (see Fig. 5 and Table 3). The figure shows three pronounced absorption lines as well as a weaker and broader line at 1.060 THz with a width of 0.4 THz which can clearly be seen for HR crystal on the

#222577 - $15.00 USD Received 8 Sep 2014; accepted 18 Sep 2014; published 10 Oct 2014

inset. The left slope of the weak line was previously demonstrated in [18] (see Fig. 3b there), however it was neither discussed nor quantified.

It can be seen from Table 3 that the frequencies of all phonon modes increase together with resistivity. This effect is also accompanied by the sharpening of the absorption lines. The refractive indices decrease with resistivity and show peculiarities attributed to the sharp phonon peaks. For example, LR crystal demonstrate refractive index higher by 0.08 compared to HR crystal in the frequency range up to 1.65 THz that is explained by a more significant contribution of the absorption line at 2.71 THz.

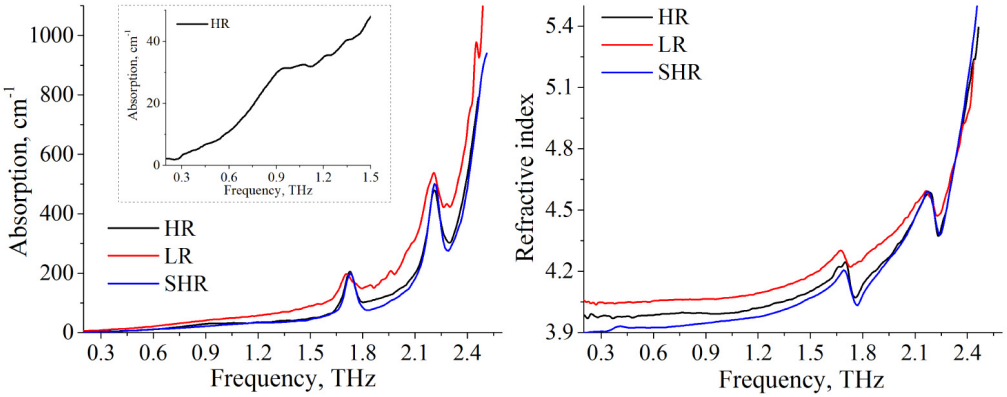

Fig. 5. Terahertz absorption (left) and refractive indices (right) of LR, HR, and SHR crystals along the *z*-axis at room temperature of 296 K.

Table 3. Comparison of characteristics of three phonon lines along *z*-axis for LR, HR and SHR crystals at room temperature

Crystal	f_1, THz	w_1, THz	A_1, 10^3 THz/m	f_2, THz	w_2, THz	A_2, 10^3 THz/m	f_3, THz	w_3, THz	A_3, 10^3 THz/m
LR	1.720	0.15	2.1	2.181	0.146	5.6	2.71*	0.27*	165*
HR	1.726	0.084	1.9	2.204	0.076	3.3	2.74*	0.08*	492*
SHR	1.729	0.061	1.5	2.208	0.067	3.5	2.72*	0.09*	358*

*Position, width and amplitude of this peak were estimated using fitting of the left slope of the absorption line.
The data in the table are presented to the last significant digit.

The results of this study, as well as the properties of KTP crystals obtained in earlier publications, are presented in Table 4. As can be seen, most of the previous results agree with those reported herein. Some of the studies conducted in the past lack axis specificity. For example, not KTP crystals but powder was examined by the usage of Fourier transform spectroscopy [16]. For this reason, the measurements found in the above work contain the absorption lines from all three KTP axes. The most comprehensive study of near- and far-infrared properties of KTP crystals was carried out using infrared reflectance spectroscopy by Kugel et. al. [15]. The authors found three very strong absorption lines (2.52 THz, 2.76 THz and 2.73 THz along *x*- *y*- and *z*-axes correspondingly) that significantly distorted IR-reflectance results at lower frequencies.

In [18], Mounaix et al. studied a KTP crystal by THz-TDS in a narrow range of 0.2 to 1.0 THz along the *y*- and *z*-axes. This explains why the authors did not observe any absorption lines. The KTP properties were also investigated by THz-TDS, presumably along the *z*-axis, in [19] by Sang et al. These studies lack our dynamic and spectral range of investigation.

#222577 - $15.00 USD Received 8 Sep 2014; accepted 18 Sep 2014; published 10 Oct 2014

Table 4. Comparison of phonon modes found in this study with previous investigations, central frequency, THz

This study, THz-TDS, HR crystal			[19], THz-TDS, axis not specified	[16], FT-IR, powder samples	[17], Raman spectroscopy			[15], IR reflectance		
x	*y*	*z*			*x*	*y*	*z*	*x*	*y*	*z*
		1.06								
		1.726	1.76	1.74			1.83			
	2.154			2.14						
		2.204					2.19	2.22	2.25	
2.439				2.31				2.4	2.4	2.36
			2.58				2.55	2.52		
2.67	2.64			2.67	2.64	2.64		2.685		
		2.74			2.76		2.76		2.76	2.73

As a part of the study, we have additionally cooled thick y-cut HR and LR crystals to 80 K and studied their terahertz optical properties (see Fig. 6). However, the absorption and reflections of terahertz radiation by cryostat windows lowered the dynamic range of the measurements, which lowered the accuracy of the results and narrowed the detected spectral range.

By fitting the corresponding absorption lines using Lorentzian approximations, the central frequencies of the phonon modes were shown to move up 30 or 50 GHz as the temperature lowered from 296 K to 80 K, while their width decreased twofold. The frequency shift between the corresponding phonon frequencies of the LR and HR crystals remained the same at about 10 GHz.

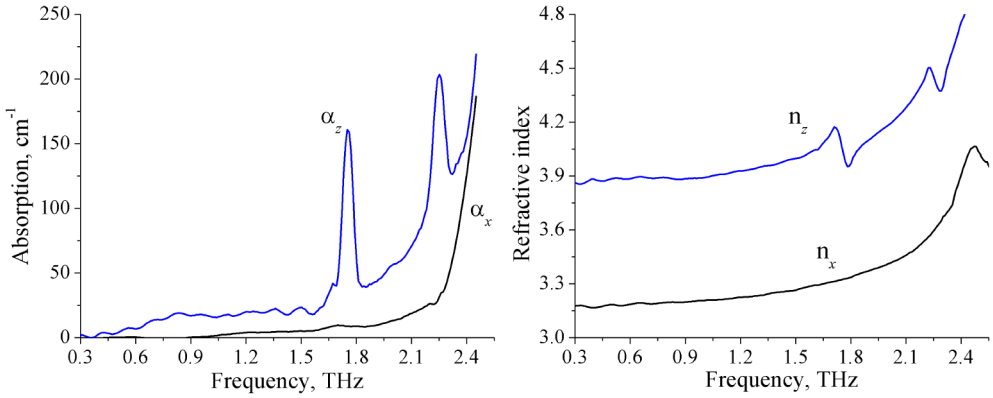

Fig. 6. Absorption and refractive indices of high-resistivity KTP crystal at 80 K.

To explain the aforementioned phenomena, we focused on the internal structure of KTP crystals. It was shown previously that vibrations with wavenumbers less than 200 cm^{-1} were attributed to the external lattice modes. These oscillations include potassium ions moving relative to the TiO_6 and PO_4 atom groups forming the basis of the KTP crystalline structure [15]. The main contributor to KTP conductivity is potassium ion movement in spiral paths along the *z*-axis [3]. This movement occurs as hopping between two crystallographically independent positions: the first one is along 9 surrounding oxygen ions (K1 position) and the other one is along 8 oxygen ions (K2 position). Electron density studies demonstrate that there are additional stable ion positions (K1′, K1″, K2′ and K2″) in vicinity of the main ones, i.e. a structural disorder is observed. Potassium ions travel easier between the additional positions that explains why vacancies at these positions allow for better hopping ion mobility.

#222577 - $15.00 USD Received 8 Sep 2014; accepted 18 Sep 2014; published 10 Oct 2014

The effectiveness of hopping is determined by the distance between different positions and their population. These parameters depend on the crystal growth conditions and change with the temperature. For example, ion hopping is frozen at the temperatures below ~200 K which is indicated by the prevalence of polaron conductivity [24]. At the same time some part of the potassium ions remain at additional positions or the potential of the main state is distorted. It was indicated in [25] by Larsen, who observed these additional ion positions for KTP at 9 K, similar to the ones existing at 293 K, although, their population was very low and was not estimated. Moreover this was demonstrated on KTA crystals isomorphous to KTP that the population of additional positions decreased but not to zero if the temperature decreased from 293 K to 30 K [26].

These considerations suggest that almost all K^+ ions in KTP crystals with high resistivity occupy the main positions, whereas additional positions are shallow or located far apart. In contrast, LR crystals have a large number of ions and ion vacancies at additional positions, hence their high conductivity. Moreover, the higher level of structural disorder in LR crystals as compared to HR crystals yields wider terahertz absorption lines. The properties of different crystals (width and position of absorption lines) were expected to become more uniform at lower temperatures because of the anticipated phase transition from ion conductivity (prevailing at T>200 K) to polaron one (characteristic of lower temperatures). On the contrary, the relations between the corresponding absorption lines in high- and low-resistive crystals at 80 K remained the same. Seemingly ions continued to occupy some of the additional positions at lower temperatures. This indicated that the potassium sublattice disorder remained in place.

4. Conclusion

For the first time, we have experimentally studied the optical properties of super-high-, high- and low-resistive nonlinear optical KTP crystals in the frequency range of 0.2 to 2.6 THz by the method of terahertz time-domain spectroscopy. The observed absorption lines were attributed to the external oscillations of potassium ions. A greater degree of disorder in the potassium sublattice (vacancies, additional positions, etc.) in the LR crystals as compared to the HR ones manifested itself in wider terahertz absorption lines and larger DC conductivity along the *z*-axis. The relation of width and frequency of the corresponding lines in the LR and HR crystals remained the same after the temperature had been lowered to 80 K. In our opinion, the observed behavior indicated that the potassium sublattice disorder persisted and influenced the terahertz properties of both LR and HR KTP crystals at lower temperatures.

Acknowledgments

The study was supported by the Russian Fund of Basic Research, Project 12-02-12027-ofi_m, the Ministry of Education and Science of the Russian Federation, Project 14.B37.21.0452, and the Presidium of the Russian Academy of Sciences, Program 24.